

Dilatancy of Remoulded Fine-grained Soils

by

Huang Lianfang

Master of Science in Civil and Environmental Engineering



2009



**Faculty of Science and Technology
University of Macau**

Dilatancy of Remoulded Fine-grained Soils

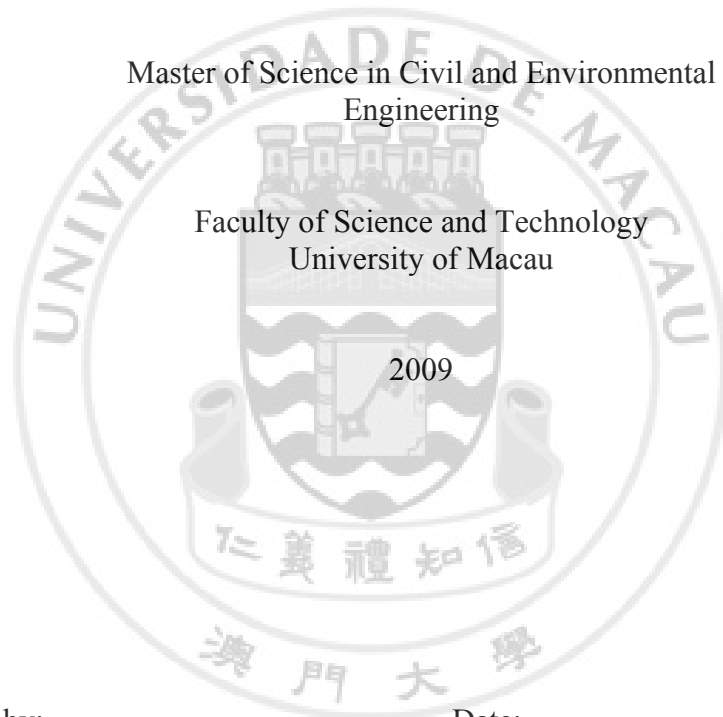
by

Huang Lianfang

A thesis submitted in partial fulfillment of the
requirements for the degree of

Master of Science in Civil and Environmental
Engineering

Faculty of Science and Technology
University of Macau



Approved by: _____ Date: _____
Supervisor: Prof. Ka Veng Yuen

Approved by: _____ Date: _____
Co-supervisor: Dr. Yan Wai Man

Accepted by: _____ Date: _____
Examiner: Dr. Lok Man Hoi

Accepted by: _____ Date: _____
Examiner: Prof. Kou Kun Pang

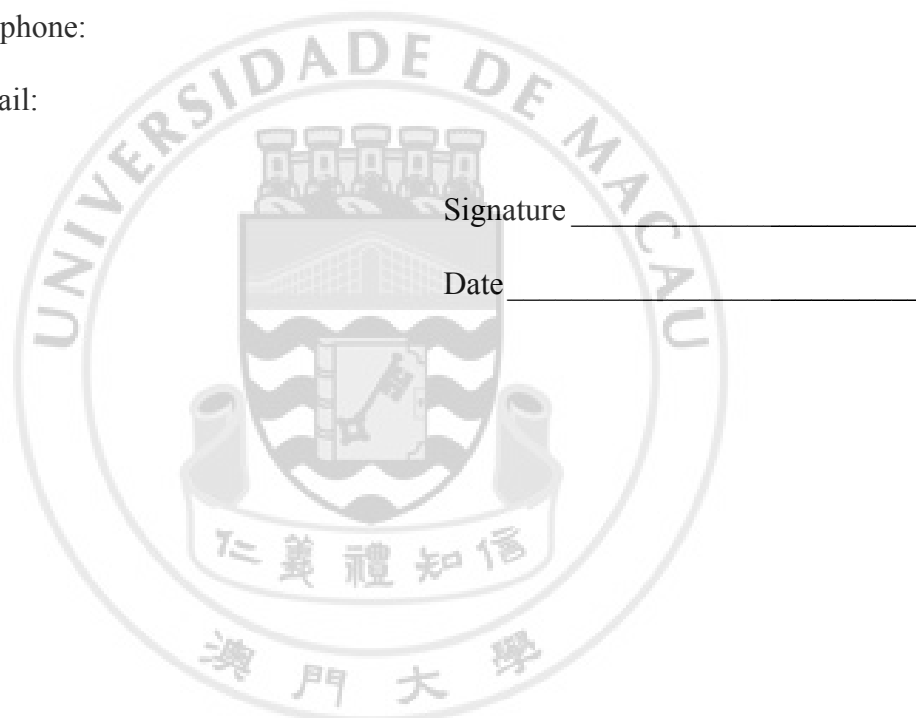
In presenting this thesis in partial fulfillment of the requirements for a Master's degree at the University of Macau, I agree that the Library and the Faculty of Science and Technology shall make its copies freely available for inspection. However, reproduction of this thesis for any purposes or by any means shall not be allowed without my written permission. Authorization is sought by contacting the author at

Address:

Telephone:

Fax:

E-mail:



ABSTRACT

Along with the development of the formulation of suitable constitutive relationships for geomaterials, dilatancy has become a common feature of the soils which studied by geotechnical engineers, and is a part of the broader topic of soil mechanics. To study the mechanical behaviour especially the dilatancy of a remoulded fine-grain soil under different stress paths in triaxial space, in this research, the investigation was performed in the laboratory with triaxial tests on remoulded kaolin clay samples. The triaxial tests included isotropic and anisotropic consolidation as well as drained and undrained triaxial compression tests. The tests data is interpreted within the framework of critical state soil mechanics. Evolution of dilatancy is evaluated under different stress paths.

During constant stress-ratio shearing, it is found that the dilatancy of the soil is not a constant but varies at the very beginning due to induced anisotropy. However, when strain becomes higher, dilatancy approaches a constant for a specific stress ratio. Soil shears under smaller η produces large dilatancy. For specimen that isotropically consolidated, the dilatancy D tends to infinity. The dilatancy of the soil during constant p' shearing and conventional drained shearing decreases as η increases and it approaches to zero as η approaches M_c .

A model for saturated soil is presented, modified from an unsaturated model for soil proposed by Li (2007). Based on the presented model, the modified Cam clay model, the original Cam clay and Rowe's stress-dilatancy relationship, the experimental findings of some laboratory triaxial tests are discussed.

The yield surface presented by the model modified from Li's unsaturated model was drawn and compared to the test results, with some calibrated or assumed model

constants. Experimental data indicate that the shape of the yield curve presented by the model modified from Li's model is a reasonable approximation for the soil.

The data from the constant η compression, constant p' shearing and conventional drained compression tests were analyzed. It is found that the model modified from Li's model gives a much better agreement than other models under constant η compression, none of these theoretical flow rules is appropriate for matching the experimental data for this soil under constant p' shearing, and the modified Cam clay model gives a much better agreement than other models for soil under conventional drained compression.



TABLE OF CONTENTS

List of figures.....	iv
List of tables	viii
Nomenclature.....	ix
Acknowledgments	x
Chapter 1: Introduction.....	1
1.1 Background.....	1
1.2 Objectives	1
1.3 Layout of This Thesis	2
Chapter 2: Literature Review	4
2.1 Anisotropy.....	4
2.2 Stress-dilatancy	6
2.2.1 Introduction.....	6
2.2.2. Flow Rule for Original Cam Clay Model	7
2.2.3 The Flow Rule for The Modified Cam Clay Model	8
2.2.4. Rowe’s Stress-Dilatancy Relation	9
2.2.5. Experimental Findings	11
Chapter 3: Experimental Set-up	22
3.1 Introduction.....	22
3.2 Description of Soil Sample	22
3.2.1 Index PropertieS.....	23
3.2.1.1 Specific Gravity G_s	23
3.2.1.2 Particles Size Distribution.....	23
3.2.1.3 Atterberg Limits.....	23
3.2.2 Remoulded sample preparation.....	23
3.3 Triaxial Testing System	24
3.3.1 CKC Triaxial System.....	25
3.3.2 Lubricated Ends	25

3.3.3 Triaxial System Calibration	26
3.3.3.1 Load Cell Calibration	27
3.3.3.2 Cell pressure and Effective pressure Calibration	27
3.3.3.3 Volume-measuring Device Calibration	27
3.3.3.4 LVDT Calibration	27
3.4 Testing Procedures	28
3.4.1 Trimming of Specimens	28
3.4.2 Triaxial Specimen Preparation	28
3.4.3 Vacuum Saturation	28
3.4.4 Back Pressure Saturation	29
3.4.5 Isotropic Consolidation	30
3.4.6 K_0 Consolidation	30
3.4.7 Deviator Shearing	30
3.4.8 Determination of Final Water Content	31
Chapter 4: Results of Triaxial Tests	38
4.1 Introduction	38
4.2 Isotropic Compression and Swelling	38
4.3 K_0 Consolidation Tests	39
4.4 Constant Stress-Ratio Shearing Tests	40
4.5 Conventional Drained and Undrained Compression Tests	42
4.6 Constant p' Shearing Tests	43
4.7 Discussions	44
Chapter 5: Analysis	61
5.1 Discussion of the experimental findings	61
5.2 A model modified from an unsaturated model proposed by Li (2007b)	62
5.2.1 Yield function and plastic flow	63
5.2.2 Elastic Relations	65
5.3 Model Behaviour	66
Chapter 6: Conclusions and Future Study	76
6.1 Overview	76
6.2 Remoulded Fine-grain Soil Behaviour in Laboratory Tests	77

6.3 Theoretical Treatment.....	78
6.4 Future Study.....	79
References.....	80



LIST OF FIGURES

Chapter 2

Fig. 2.1 Stress ratio $\eta = q/p'$ and the plastic dilatancy $D = \delta\varepsilon_v^p / \delta\varepsilon_q^p$ (modified from Wood, 1990).....	17
Fig. 2.2 Plastic strain increments for isotropic compression and critical states plotted in p' - q effective stress plane (modified from Wood, 1990).....	17
Fig. 2.3 Stress-dilatancy relationships: (1) modified Cam clay, (2) original Cam clay, (3) Rowe's stress-dilatancy (drawn for $M = 1$) (modified from Wood, 1990)..	18
Fig. 2.4 Plastic potentials: (1) modified Cam clay, (2) original Cam clay, (3) Rowe's stress-dilatancy (drawn for $M = 1$) (modified from Wood, 1990).....	18
Fig. 2.5 Plastic potential for modified Cam clay model (drawn for $M = 1$) (modified from Wood, 1990).....	19
Fig. 2.6 Data from conventional drained triaxial compression tests (●, medium sand; +, quartz silt; ×, feldspar) stress-dilatancy relationships: (1) modified Cam clay, (3) Rowe's stress-dilatancy (data from Rowe, 1971) (Wood, 1990).....	19
Fig. 2.7 Data from conventional drained (○) and undrained (●) triaxial compression tests on isotropically normally compressed spestone kaolin [stress-dilatancy relationships: (1) modified Cam clay, (2) original Cam clay] (data from Roscoe et al., 1963) (Wood, 1990).....	20
Fig. 2.8 Stress-dilatancy relationships for Llyn Brianne slate dust: (○) isotropically compressed; and (●) one-dimensionally compressed (data from Lewin, 1973) (Wood, 1990).....	20
Fig. 2.9 Vectors of plastic strain increment plotted at yield points deduced from triaxial tests on undisturbed Winnipeg clay (data from Graham et al., 1983) (Wood, 1990).....	21
Fig. 2.10 Stress-dilatancy relationships observed for undisturbed Winnipeg clay (data from Graham et al., 1983) (Wood, 1990).....	21

Chapter 3

Fig. 3.1 Testing procedures for gradation curve.....	32
Fig. 3.2 Particle size distribution of the soil.....	32
Fig. 3.3 Remolded sample preparation.....	33
Fig. 3.4 CKC triaxial testing system.....	34
Fig. 3.5 Sketch of lubricated ends.....	35
Fig. 3.6 End plates of CKC triaxial cell.....	35
Fig. 3.7 LVDT calibration.....	36
Fig. 3.8 Triaxial specimens trimming device.....	37

Chapter 4

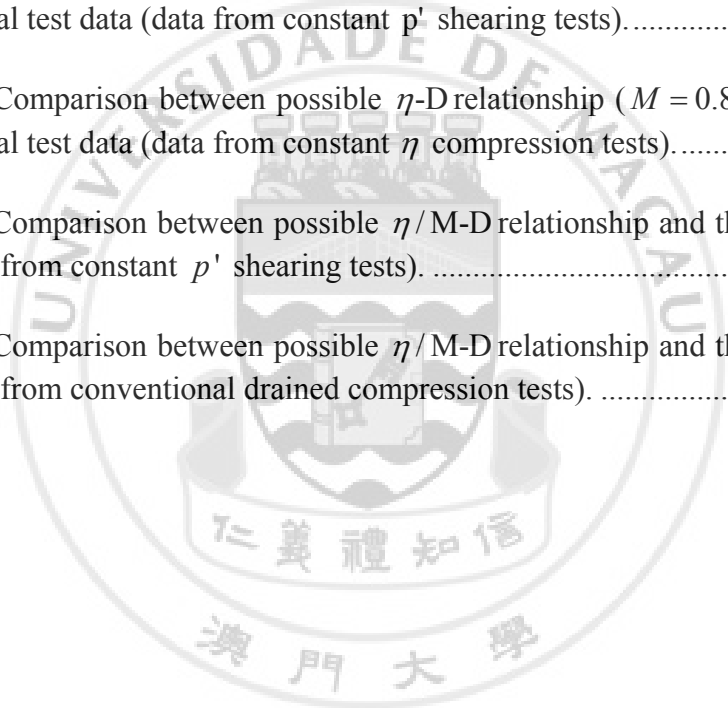
Fig. 4.1 Isotropic consolidation lines in an e - $\ln p'$ space.....	48
Fig. 4.2 Variations of strains during isotropic loading (ISO 02).....	48
Fig. 4.3 Variations of axial strain with radial strain during isotropic compression.....	49
Fig. 4.4 The volumetric strain ε_v against deviatoric strain ε_q during the K_0 consolidation tests.....	49
Fig. 4.5 Stress paths used to study the dilatancy during a specific stress ratio.....	50
Fig. 4.6 Constant stress-ratio compression lines in an e - $\ln p'$ space.....	50
Fig. 4.7 Volumetric strain ε_v against deviatoric strain ε_q during the constant stress-ratio testing.....	51
Fig. 4.8 Plastic volumetric strain increment $\delta\varepsilon_v^p$ against plastic deviatoric strain increment $\delta\varepsilon_q^p$ during the constant stress-ratio testing.....	51
Fig. 4.9 The variations of strains during constant η shearing.....	52

Fig. 4.10 The response of the specimens under conventional drained compression test at $p_0' = 300kPa$	53
Fig. 4.11 The response of the specimens under conventional undrained compression test at $p_0' = 300kPa$	54
Fig. 4.12 ε_v ($\delta\varepsilon_v^p$) against ε_q ($\delta\varepsilon_q^p$) during the conventional drained shearing testing.....	55
Fig. 4.13 ε_v ($\delta\varepsilon_v^p$) against ε_q ($\delta\varepsilon_q^p$) during the conventional undrained shearing testing.....	55
Fig. 4.14 The variation of dilatancy ($\delta\varepsilon_v^p/ \delta\varepsilon_q^p $) with stress ratio η during conventional drained shearing test.....	56
Fig. 4.15 The response of the specimens during constant p' shearing tests.....	56
Fig. 4.16 Volumetric strain ε_v against axial strain ε_a during the constant p' testing	57
Fig. 4.17 The variation stress ratio η during constant p' shearing against ε_a	57
Fig. 4.18 The variation of $\delta\varepsilon_v/ \delta\varepsilon_q $ during constant p' shearing against ε_a	58
Fig. 4.19 The variation of $\delta\varepsilon_v/ \delta\varepsilon_q $ with stress ratio η during constant p' shearing.....	58
Fig. 4.20 CSL of triaxial compression in p' - q space.	59
Fig. 4.21 CSL of triaxial compression in e - $\ln p'$ space.	59
Fig. 4.22 The variations of η_{cr} with p_{cr}' for triaxial compression tests.	60

Chapter 5

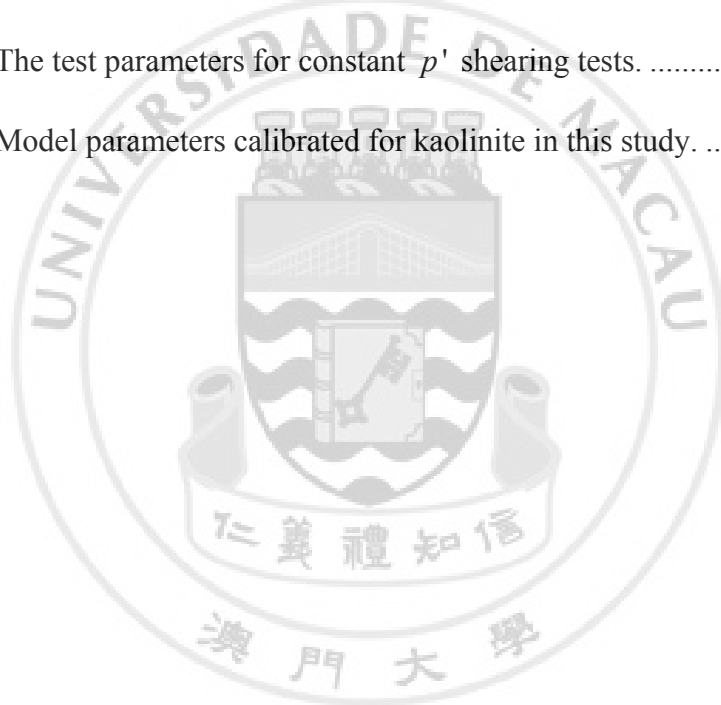
Fig. 5.1 The variations of D with p' for the constant η shearing tests ($\eta = 0.2$). ...	68
Fig. 5.2 The variations of D with p' for the constant η shearing tests ($\eta = 0.4$). ...	69
Fig. 5.3 The variations of D with p' for the constant η shearing tests ($\eta = 0.6$). ...	69

Fig. 5.4 The variations of the dilatancy with different stress-ratio η in constant stress-ratio shearing tests ($M=0.8$).....	70
Fig. 5.5 The variations of the dilatancy with η/M in constant p' shearing tests.	70
Fig. 5.6 The variations of the dilatancy with η/M in conventional drained compression tests.	71
Fig. 5.7 Yield surface in a triaxial true stress space.....	71
Fig. 5.8 Yield point evaluation method.	72
Fig. 5.9 Comparison between possible yield surface ($M = 0.8, \alpha = 0.6$) and the triaxial test data (data from constant p' shearing tests).....	72
Fig. 5.10 Comparison between possible η -D relationship ($M = 0.8, \alpha = 0.6$) and the triaxial test data (data from constant η compression tests).....	73
Fig. 5.11 Comparison between possible η/M -D relationship and the triaxial test data (data from constant p' shearing tests).....	74
Fig. 5.12 Comparison between possible η/M -D relationship and the triaxial test data (data from conventional drained compression tests).	75




LIST OF TABLES

Table 4.1 The test parameters for isotropic compression and swelling tests.....	45
Table 4.2 The test parameters for K_o consolidation tests.	45
Table 4.3 The test parameters for constant stress ratio shearing tests.	46
Table 4.4 The test parameters for conventional drained and undrained compression tests.	46
Table 4.5 The test parameters for constant p' shearing tests.	47
Table 5.1 Model parameters calibrated for kaolinite in this study.	68



NOMENCLATURE



ψ	state parameter
$\Gamma_{cr}, \lambda_{cr}$	parameters associated with the critical state line in $e-\ln p'$ plane
D	dilatancy
e	void ratio
G	elastic shear modulus
G_s	specific gravity
K	elastic bulk modulus
M	critical stress ratio for triaxial compression
ν	Poisson's ratio
w	water content
ε_a	axial strain
ε_q	deviatoric strain
ε_r	radial strain
ε_v	volumetric strain
η	stress ratio, q/p'
κ	isotropic unloading slope in $e-\ln p'$ plane
σ_a	axial stress in triaxial test
σ_r	radial stress in triaxial test

ACKNOWLEDGMENTS

Dr. Yan Wai Man offered me the opportunity of postgraduate study at the Department of Civil and Environmental Engineering in University of Macau. I would like to thank my co-supervisor supervisor Dr. Yan Wai Man very much for this outstanding initiative. I would like to express my deepest gratitude to my research supervisor, Prof. Ka Veng Yuen and co-supervisor supervisor, Dr. Yan Wai Man for their consistent support, guidance and understanding during my research period. They also have walked me through all the stages of the writing of this thesis. Without their consistent and illuminating instruction, this thesis could not have reached its present form.

I would like to thank Dr. Lok Man Hoi and Prof. Kou Kun Pang, for their valuable teaching, discussions and comments on my research project.

Mr. Sein Ye Htut, Edward, technician of the Geotechnical Laboratory, gave essential support at every phase of the project.

Many thanks go to my friends Ma Yongfeng, Lan Shuangwen, Liu Xinglu, Feng Yu, Zhang He and Sun Jie for their supports.

My special thanks go also to all those colleagues and friends who are not named explicitly in here, but who supported me a lot during the preparation of this thesis.

Last, but not least, I particularly would like to thank my family for their encouragement and mental support throughout all these years.